ARTICLE

De Novo Missense Mutations in *DHX30* Impair Global Translation and Cause a Neurodevelopmental Disorder

Davor Lessel,[1,2,28,29,*] Claudia Schob,[1,28,29] Sébastien Küry,[3] Margot R.F. Reinders,[4] Tamar Harel,[5] Mohammad K. Eldomery,[6] Zeynep Coban-Akdemir,[6] Jonas Denecke,[7] Shimon Edvardson,[8,9] Estelle Colin,[10,11] Alexander P.A. Stegmann,[4,12] Erica H. Gerkes,[13] Marine Tessarech,[10,11] Dominique Bonneau,[10,11] Magalie Barth,[10,11] Thomas Besnard,[3] Benjamin Cogné,[3] Anya Revah-Politi,[14] Tim M. Strom,[15,16] Jill A. Rosenfeld,[6] Yaping Yang,[6] Jennifer E. Posey,[6] LaDonna Immken,[17] Nelly Oundjian,[18] Katherine L. Helbig,[19] Naomi Meeks,[20,21] Kelsey Zegar,[20,21] Jenny Morton,[22] the DDD study, Jolanda H. Schieving,[23] Ana Claasen,[24] Matthew Huentelman,[24] Vinodh Narayanan,[24] Keri Ramsey,[24] C4RCD Research Group, Han G. Brunner,[4] Orly Elpeleg,[5,9] Sandra Mercier,[3] Stéphane Bézieau,[3] Christian Kubisch,[1,2] Tjitske Kleefstra,[4] Stefan Kindler,[1] James R. Lupski,[6,25,26,27] and Hans-Jürgen Kreienkamp[1,*]

DHX30 is a member of the family of DExH-box helicases, which use ATP hydrolysis to unwind RNA secondary structures. Here we identified six different *de novo* missense mutations in *DHX30* in twelve unrelated individuals affected by global developmental delay (GDD), intellectual disability (ID), severe speech impairment and gait abnormalities. While four mutations are recurrent, two are unique with one affecting the codon of one recurrent mutation. All amino acid changes are located within highly conserved helicase motifs and were found to either impair ATPase activity or RNA recognition in different *in vitro* assays. Moreover, protein variants exhibit an increased propensity to trigger stress granule (SG) formation resulting in global translation inhibition. Thus, our findings highlight the prominent role of translation control in development and function of the central nervous system and also provide molecular insight into how DHX30 dysfunction might cause a neurodevelopmental disorder.

Introduction

ATP-dependent unwinding of RNA secondary structures by RNA helicases (RHs) is required for most aspects of RNA metabolism, including synthesis, nuclear processing and export, translation, and storage and decay of RNA, as well as ribonucleoprotein (RNP) assembly.[1–3] Six superfamilies of RHs are known,[2] with superfamily 2 containing more than 50 human members characterized by a DExD or DExH signature in their Walker B motif, thus termed DDX and DHX proteins, respectively.[4] Several RHs have been assigned to multiple cellular functions, often operating in large RNP complexes, while others appear to be restricted to a particular cellular process.[2] Whereas a large body of structural and functional data has been accumulated for RHs from model organisms, such as the yeast DExH protein Prp43, for most human RHs the exact function remains unknown.

Human genetic studies have recently begun to address the pathological relevance of altered RH function; thus, somatic mutations in *DDX3X* (MIM: 300160) observed in various tumors were found to disrupt global translation.[5]

[1]Institute of Human Genetics, University Medical Center Hamburg-Eppendorf, 20246 Hamburg, Germany; [2]Undiagnosed Disease Program at the University Medical Center Hamburg-Eppendorf (UDP-UKE), Martinistraße 52, 20246 Hamburg, Germany; [3]CHU Nantes, Service de Génétique Médicale, 9 quai Moncousu, 44093 Nantes Cedex, France; [4]Department of Human Genetics, Radboud University Medical Center, 6500 HB Nijmegen, the Netherlands; [5]Department of Genetic and Metabolic Diseases, Hadassah-Hebrew University Medical Center, Jerusalem, Israel 9112001; [6]Department of Molecular and Human Genetics, Baylor College of Medicine, Houston, TX 77030, USA; [7]Department of Pediatrics, University Medical Center Eppendorf, 20246 Hamburg, Germany; [8]Pediatric Neurology Unit, Hadassah-Hebrew University Medical Center, Jerusalem, Israel 9112001; [9]Monique and Jacques Roboh Department of Genetic Research, Hadassah-Hebrew University Medical Center, Jerusalem, Israel 9112001; [10]Department of Biochemistry and Genetics, University Hospital, 49933 Angers Cedex 9, France; [11]Equipe MitoLab, CNRS UMR 6015, Inserm U1083, Institut MitoVasc of Angers, CHU Bât IRIS/IBS, Rue des Capucins, 49933 Angers Cedex, France; [12]Department of Clinical Genetics, Maastricht University Medical Centre, Maastricht, the Netherlands; [13]Department of Genetics, University of Groningen, University Medical Center Groningen, Groningen, the Netherlands; [14]Institute for Genomic Medicine, Columbia University, New York, NY 10032, USA; [15]Institute of Human Genetics, Helmholtz Zentrum München, 85764 Neuherberg, Germany; [16]Institute of Human Genetics, Technical University of Munich, 81675 Munich, Germany; [17]Clinical Genetics, Specially for Children, Austin, TX 78723, USA; [18]Valley Hospital, Ridgewood, NJ, USA; [19]Division of Clinical Genomics, Ambry Genetics, Aliso Viejo, California, USA; [20]Division of Clinical Genetics and Metabolism, Department of Pediatrics, University of Colorado School of Medicine, Aurora, CO, USA; [21]Clinical Genetics, Children's Hospital Colorado, Aurora, CO, USA; [22]West Midlands Regional Clinical Genetics Service and Birmingham Health Partners, Birmingham Women's and Children's NHS Foundation Trust, B15 2TG Birmingham, UK; [23]Department of Pediatric Neurology, Donders Institute for Brain, Cognition and Behaviour, Radboud University Medical Center, Nijmegen, the Netherlands; [24]Center for Rare Childhood Disorders, Translational Genomics Research Institute, Phoenix, Arizona, USA; [25]Texas Children's Hospital, Houston, TX 77030, USA; [26]Baylor Genetics Laboratories, Baylor College of Medicine, Houston, TX 77030, USA; [27]Human Genome Sequencing Center, Baylor College of Medicine, Houston, TX 77030, USA
[28]First author
[29]These authors contributed equally to this work
*Correspondence: d.lessel@uke.de (D.L.), kreienkamp@uke.de (H.-J.K.)
https://doi.org/10.1016/j.ajhg.2017.09.014.

Moreover, germline mutations in the same gene are associated with intellectual disability (MIM: 300958),[6] pointing to a role of translational control in proper development and function of the nervous system.

Here we describe disease-causing *de novo* missense mutations in *DHX30* (MIM: 616423, RefSeq NM_138615.2) in individuals affected by intellectual disability and global developmental delay. DHX30 belongs to the DExH family of RNA helicases, and has until now mostly escaped scientific attention. We show that DHX30 is indeed an RNA-dependent ATPase, and that all mutations interfere with either RNA binding or ATPase activity. Importantly, protein variants of DHX30 interfere also with global translation by inducing the formation of stress granules.

Material and Methods

Research Subjects

Written informed consent for all subjects was obtained in accordance with protocols approved by the respective ethics committees of the institutions involved in this study.

Genetic Analysis

Some of the investigators presenting affected individuals in this study were connected through GeneMatcher, a web-based tool for researchers and clinicians working on identical genes.[7] Trio whole-exome sequencing (trio-WES) experiments, data annotation, and interpretation were performed in nine different centers with slightly different procedures using methods that were described previously. Briefly, trio-WES in families A, C, D, E, J, and L were performed with a SureSelect Human All Exon (Agilent, Santa Clara, CA, USA), and sequenced on a HiSeq2000, HiSeq2500 or HiSeq4000 platform (Illumina, San Diego, CA, USA), as described before.[8–13] Trio-WES in families B, H, and K was performed with a SOLiD-Optimized SureSelect Human Exome Kit (Agilent version 2, 50 Mb), followed by SOLiD 4 System sequencing (Life Technologies) as previously described.[14,15] Trio-WES in family I was performed using the SeqCapEZ VCR 2.0 (Roche NimbleGen) and sequenced on the HiSeq 2000 Sequencer (Illumina, San Diego, CA, USA) as previously described.[16] Genetic analyses in families F and G were described before.[17] All putative *de novo* variants were validated and confirmed by Sanger sequencing, by standard procedure.

Expression Constructs

cDNA coding for transcript variant 1 of human DHX30 was obtained from Origene; the DHX30 coding sequence was subcloned into EcoRI/SmaI sites of pEGFP-C3 (Clontech), allowing for expression of DHX30-WT carrying an N-terminal GFP-tag (GFP-DHX30). In parallel, several constructs were generated in pEGFP-N2, leading to expression of DHX30 variants carrying a C-terminal GFP-tag (DHX30-GFP); in particular, we generated a construct corresponding to transcript variant 3; the protein product of this cDNA carries a putative N-terminal mitochondrial targeting sequence. Missense mutations found in affected individuals were introduced into the pEGFP-C3 based vector, and into the mitochondrial construct using Quick-Change II site directed mutagenesis kit (Agilent, Waldbronn, Germany), with mutagenic oligonucleotides designed based on the Quick-Change instruction manual. All constructs were verified by Sanger sequencing.

Cell Culture, Transfection, and Immunocytochemistry

Human embryonic kidney 293T (HEK293T) and human bone osteosarcoma epithelial (U2OS) cells were grown on cell culture dishes and coverslips, respectively, utilizing Dulbecco's Modified Eagle Medium (DMEM) supplemented with 10% fetal bovine serum (FBS). Cells were transfected with TurboFect transfection reagent (ThermoFisher Scientific) according to the manufacturer's recommendations. Fixation of U2OS cells and immuno-cytochemical analysis was performed as previously described[18] employing the following antibodies at manufacturers' recommended dilutions: anti-DHX30 rabbit polyclonal (Bethyl, #A302-218A), anti-DDX3X mouse monoclonal (BioLegend, #658602), anti-Mitochondria mouse monoclonal (Abcam, #ab3298), anti-puromycin mouse monoclonal (Millipore, #MABE343), and goat anti-mouse, anti-rat, and anti-rabbit IgG coupled to either Alexa Fluor 488, Alexa Fluor 546, or Alexa Fluor 635, respectively (ThermoFisher Scientific). A custom made anti-ATXN2 rat monoclonal antibody was used at a 1:10 dilution. Recombinant DHX30 fusion proteins were directly visualized via their GFP-tag. Coverslips were mounted with ProLong Diamond Antifade Mountant with DAPI (ThermoFisher Scientific). Images were acquired utilizing a confocal microscope (Leica TCS SP8, 63x/1.25 objective) and processed using ImageJ, Corel Paint Shop Pro X, macromedia FreeHand MX and PowerPoint software.

ATPase Assay

Transfected HEK293T cells were lysed in 1 mL of radioimmunoprecipitation assay (RIPA) buffer (50 mM Tris-HCl pH 8.0; 150 mM NaCl; 0.1% SDS; 0.5% sodium deoxycholate; 1% NP-40; 5 mM EDTA) and lysates were cleared by centrifugation at 20,000 x g for 20 min at 4°C. GFP-containing proteins were purified from the supernatant by immunoprecipitation using 20 μl of GFP-Trap_A matrix (Chromotek, Munich, Germany). Precipitates were washed twice in RIPA buffer, and twice in phosphate free ATPase assay buffer (40 mM KCl; 35 mM HEPES pH 7.5; 5 mM $MgCl_2$; prepared in plastic ware to avoid phosphate contamination). Precipitates were then incubated in 50 μl phosphate free buffer supplemented with 2 mM ATP and 2 mM DTT at 30°C for 30 min (for assaying ATPase activity in the absence of exogenous RNA). After brief centrifugation (1 min, 1000 x g), the supernatant was removed and precipitate samples were incubated in phosphate free buffer containing 2 mM ATP; 2 mM DTT, and 100 μg/ml yeast RNA for 30 min at 30°C (for assaying ATPase activity in the presence of exogenous RNA). The amount of free phosphate released by ATP hydrolysis was determined photometrically using Biomol Green reagent (Enzo Life Sciences, Lörrach, Germany). Subsequently, the amount of bead-attached DHX30 protein was determined by western blotting using anti-GFP (Covance). In each case, ATPase activity was normalized to the amount of GFP-tagged DHX30 protein attached to the GFP-trap matrix.

RNA Immunoprecipitation

Immunoprecipitation of recombinant proteins from lysates of transfected HEK293T cells via GFP-Trap_A (Chromotek), RNA purification from precipitates and real-time PCR with TaqMan probes were essentially performed as previously described.[18] TaqMan Gene Expression Assays (ThermoFisher Scientific) for the

Table 1. Clinical Characteristics of Affected Individuals with *DHX30* Alterations

Clinical findings	Proband A	Proband B	Proband C	Proband D	Proband E	Proband F	Proband G	Proband H	Proband I	Proband J	Proband K	Proband L
Sex	Female	Male	Female	Female	Male	Female	Female	Female	Female	Male	Female	Male
Age at last examination (years)	3 9/12	13	6 3/12	8	17	14	14 2/12	8	6 1/12	4 8/12	6 5/12	4 8/12
Intellectual disability	+	+	+	+	+	+	+	+	+	+	+	+
Age of first words (years)	1 8/12	4	–	–	–	–	–	–	–	–	–	–
Speech ability	20 words	4 words	non-verbal	non-verbal	non-verbal	non-verbal	non-verbal	non-verbal	non-verbal	non-verbal	non-verbal	non-verbal
Motor development delay	+	+	+	+	+	+	+	+	+	+	+	+
Muscular hypotonia	+	+	+	+	+	+	+	+	+	+	+	+
Age of walking (years)	2 8/12	6	–	–	6	–	3	–	–	–	5	8
Gait abnormalities	ataxic	ataxic	no independent walking	no independent walking	ataxic; only short distances independent	no independent walking	ataxic	no independent walking	no independent walking	no independent walking	ataxic	ataxic
Autistic features	+	–	+	–	+	+	+	–	+	–	+	–
Sleep disturbance	+	+	+	+	–	–	+	+	+	–	–	–
Seizures	+	–	–	+	–	–	–	–	+	–	–	–
Feeding difficulties	+	+	–	–	+	+	+	+	+	+	–	+
Strabismus	+	–	+	–	–	–	–	–	+	+	+	+
Joint hypermobility	+	–	+	–	+	+	–	–	+	–	+	–
Cerebral MRI anomalies	–	–	–	delayed myelination, cerebellar atrophy, enlarged ventricles	cortical atrophy, dilated ventricles	mild cerebral atrophy	delayed myelination	cerebral atrophy, delayed myelination, dilated ventricles	cerebral atrophy	delayed myelination, dilated ventricles, corpus callosal abnormalities	delayed myelination, cerebellar atrophy, dilated ventricles	delayed myelination, cerebellar atrophy, dilated ventricles
***DHX30* alteration**	c.1478G>A p.Arg493His	c.1478G>A p.Arg493His	c.1685A>G p.His562Arg	c.2342G>A p.Gly781Asp	c.2342G>A p.Gly781Asp	c.2344C>T p.Arg782Trp	c.2344C>T p.Arg782Trp	c.2344C>T p.Arg782Trp	c.2353C>T p.Arg785Cys	c.2353C>T p.Arg785Cys	c.2353C>T p.Arg785Cys	c.2354G>A p.Arg785His

+, present; –, absent;

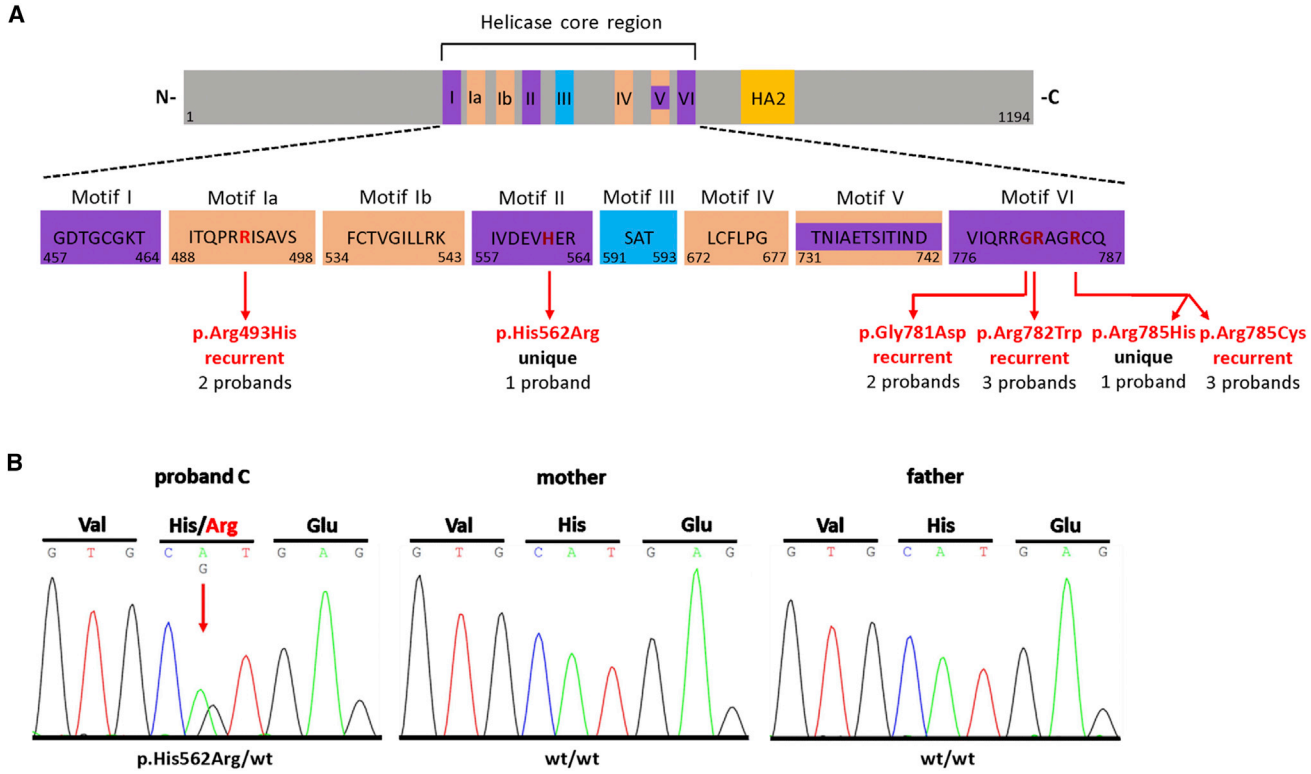

Figure 1. Identified Variants Are Localized within Conserved Helicase Motifs of DHX30
(A) Top: Schematic protein structure of DHX30 showing conserved motifs of the helicase core region and the helicase associated domain (HA2). Nucleotide-interacting motifs (I, II, and VI) are shown in purple, nucleic acid-binding motifs (Ia, Ib, and IV) in orange, motif V, which binds nucleic acid and interacts with nucleotides, in purple and orange, and motif III, which couples ATP hydrolysis to RNA unwinding, in blue. (N- N terminus; C- C terminus). Bottom: Amino acids within conserved motifs of the helicase core region. The position of the first and last amino acid within each motif is denoted below left and right, respectively. The position of the *de novo* mutations identified in this study are marked with vertical red arrows and shown in red.
(B) Sanger sequence electropherograms of parts of *DHX30* after PCR amplification of genomic DNA of the affected individual C and his parents, exemplifying *de novo* status of the mutations identified here. The amino acid translation is shown in the three-letter code above the DNA sequence. The red arrow indicates the heterozygous mutation at c.1685A>G, (p.His562Arg), present only in the DNA sample of the affected individual.

following human genes were used: *AES* (Assay ID Hs01081012_m1), *B4GAT1* (Hs04194311_s1) and *MRPL11* (Hs00601653_g1).

Puromycin Incorporation Assay

Transfected U2OS cells were pulse labeled with puromycin (Invitrogen; 1 μg/ml) for 30 min. Immuno-cytochemistry was performed as described above.

Statistics

Statistical evaluation was performed depending on the experiment by either two-tailed unpaired Student's t test or ANOVA followed by Dunnett's multiple comparisons test using Prism 6 (GraphPad), as specifically indicated for each experiment in figure legends. P values expressed as *($p < 0.05$), **($p < 0.01$), and ***($p < 0.001$) were considered significant. ns, indicates no significant difference between the groups.

Results

Using trio whole-exome sequencing (WES) or in a single case using singleton-WES followed by targeted Sanger-resequencing, we identified six different *de novo* mutations in *DHX30* in 12 unrelated individuals affected by GDD and ID. Individuals A and B spoke 20 and 4 words, respectively, whereas the others remained non-verbal. All individuals had delayed milestones of motor development. Six have never learned to walk without support, whereas the others have an ataxic gait and are only able to walk short distances. Further, subtle and only partially overlapping facial dysmorphisms were observed. The clinical phenotype further included muscular hypotonia in all affected individuals, feeding difficulties and brain anomalies on MRI in nine, autistic features and sleep disturbances in seven, and strabismus and joint hypermobility in six individuals (Figure S1, Table 1 and Supplemental Note).

DHX30 belongs to the DExH family of RHs. Within its helicase core region, there are eight highly conserved motifs which are, based on homology to other superfamily 2 helicases,[19] predicted to mediate either ATP binding/hydrolysis or RNA recognition (Figure 1 and Figure S2). Interestingly, each mutation reported herein leads to a substitution of a conserved residue within one of these motifs. We predicted the functional relevance of these residues based on homology to other superfamily 2 helicases[19] and on published structures of the RH Prp43.[20] In more detail, c.1478G>A, (p.Arg493His) identified in two individuals affects motif Ia, and Arg493 is likely a key residue mediating RNA binding.[1] All other amino acid substitutions identified lie within motifs

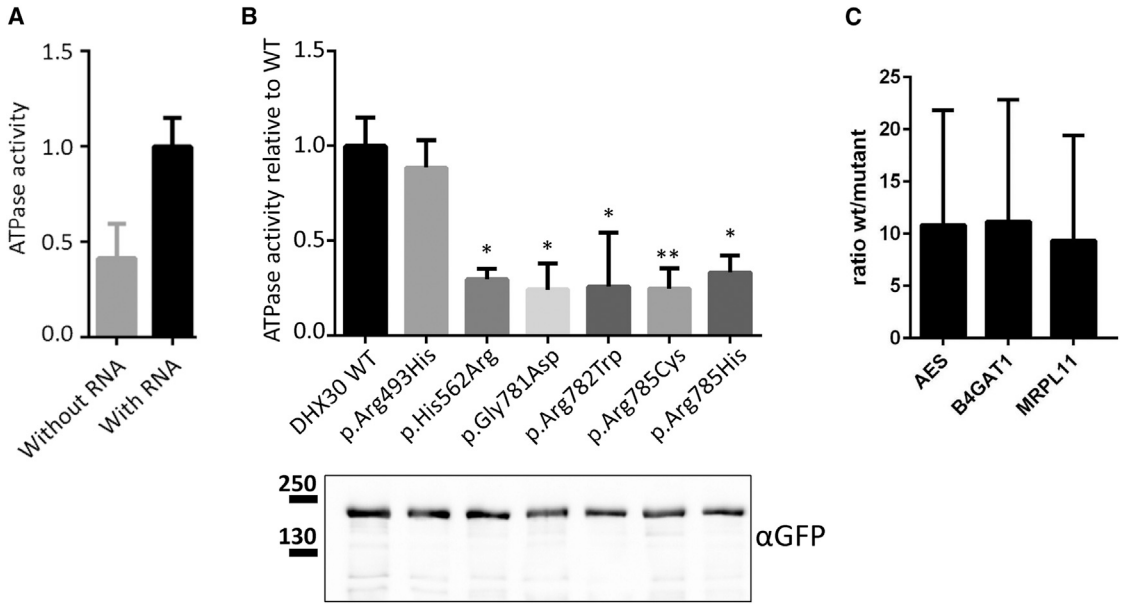

Figure 2. Recombinant Protein Variants of DHX30 Affect Either ATPase Activity or RNA-Binding
(A) GFP-tagged DHX30-WT was immunoprecipitated from HEK293T cell lysates using GFP-Trap_A matrix and assayed for ATPase activity first in the absence and then in the presence of exogenous RNA. Values are normalized on ATPase activity obtained with RNA.
(B) ATPase assays were repeated for WT and protein variants of GFP-DHX30 in the presence of RNA. In each case, ATPase activity was normalized to the amount of DHX30 protein, as determined by western blotting using anti-GFP. *,**: significantly different from DHX30-WT (*$p < 0.05$; **$p < 0.01$; $n = 4$; ANOVA, followed by Dunnett's multiple comparisons test).
(C) RNAs extracted from GFP-Trap_A precipitates of DHX30-WT, p.Arg493His, and GFP-mCherry fusion proteins obtained from transfected HEK293T cells were subjected to gene-expression analysis using TaqMan probes for specific human mRNAs. The bar graph displays the fold enrichment of *AES*, *B4GAT1*, and *MRPL11* transcripts, respectively, in DHX30-WT compared to p.Arg493His precipitates. Vertical lines indicate SD.

which we predicted to be responsible for ATP binding and/or hydrolysis. Namely, c.1685A>G, (p.His562Arg) identified in a single individual affects motif II, also referred to as Walker B motif, which binds β and γ phosphate and coordinates ATP hydrolysis.[19] Further, c.2342G>A, (p.Gly781Asp), identified in two individuals, c.2344C>T, (p.Arg782Trp), identified in three individuals, c.2353C>T, (p.Arg785Cys), also identified in three individuals, and c.2354G>A, (p.Arg785His), unique, all result in amino acid alterations residing in motif VI that binds γ phosphate and coordinates, together with motifs I and II, ATP binding and hydrolysis in other DExH family members[19,21] (Figure 1). Indeed, both Arg782 and Arg785 correspond to arginine residues that directly contact the γ phosphate.[1] Further evidence for the functional relevance of these highly conserved residues comes from *in vivo* analyses of the RH Prp43 in *Saccharomyces cerevisiae*. Substitutions of Arg150 and His218, the corresponding residues in the yeast protein to Arg493 and His562 in human DHX30 (Figure S2B), results in a cold sensitive growth retardation.[22,23] Similarly, the separate exchange of either Gly426, Arg427, and Arg430, corresponding to Gly781, Arg782, and Arg785 in DHX30, respectively (Figure S2B), is lethal.[22]

In line with the functional importance of the six residues affected in our allelic series, it is worth noting that all *DHX30* mutations identified herein are exceedingly rare; none of them is present in dbSNP, 1000 Genomes, or the ExAC or the gnomAD browser, indicating that they represent rare variants. In addition, based on the ExAC sequencing data, *DHX30* is predicted to be very intolerant to missense mutations, ranked 31 out of 18.000 analyzed genes by its missense *Z* score of 6.82,[24] which is even higher than the average *Z* score for genes involved in developmental disorders.[25] Taken together, the genetic data, especially the recurrence of mutations, supported by published structural and functional data on other RHs provide strong evidence for the pathogenicity of the identified mutations.

During murine embryogenesis, *Dhx30/HelG* is strongly expressed in neural cells, and its biallelic loss leads to perinatal lethality in mice exhibiting early development defects in the central nervous system.[26] Therefore, *DHX30* constitutes an excellent candidate gene for human neurodevelopmental disorders. In an international large-scale sequencing study, we recently reported four of the individuals presented herein and suggested *DHX30* to be a plausible candidate gene for developmental disorders.[17] However, given the large size of the previous study, the corresponding clinical picture remained unclear, and none of the reported alterations was scrutinized by an experimental approach.

Therefore, to corroborate our findings, we developed an ATPase assay using transiently transfected HEK293T cells. To assess whether wild-type DHX30 (DHX30-WT) acts as an RNA-dependent ATPase, we immunoprecipitated DHX30-GFP and incubated it with ATP in the presence or absence of RNA. Indeed, ATPase activity, determined by a progressive increase of free phosphate concentration *in vitro*, was significantly stimulated by adding RNA, thus showing that DHX30 hydrolyses ATP in an RNA-dependent fashion (Figure 2A). When compared to DHX30-WT, all protein variants harboring amino acid substitutions in ATP binding motifs II and VI (p.His562Arg, p.Gly781Asp, p.Arg782Trp, p.Arg785Cys, and p.Arg785His) exhibit markedly reduced ATPase activities (Figure 2B). These data confirm our structural predictions and provide strong evidence for the pathogenicity of the respective mutations. Noteworthy, the p.Arg493His amino acid exchange

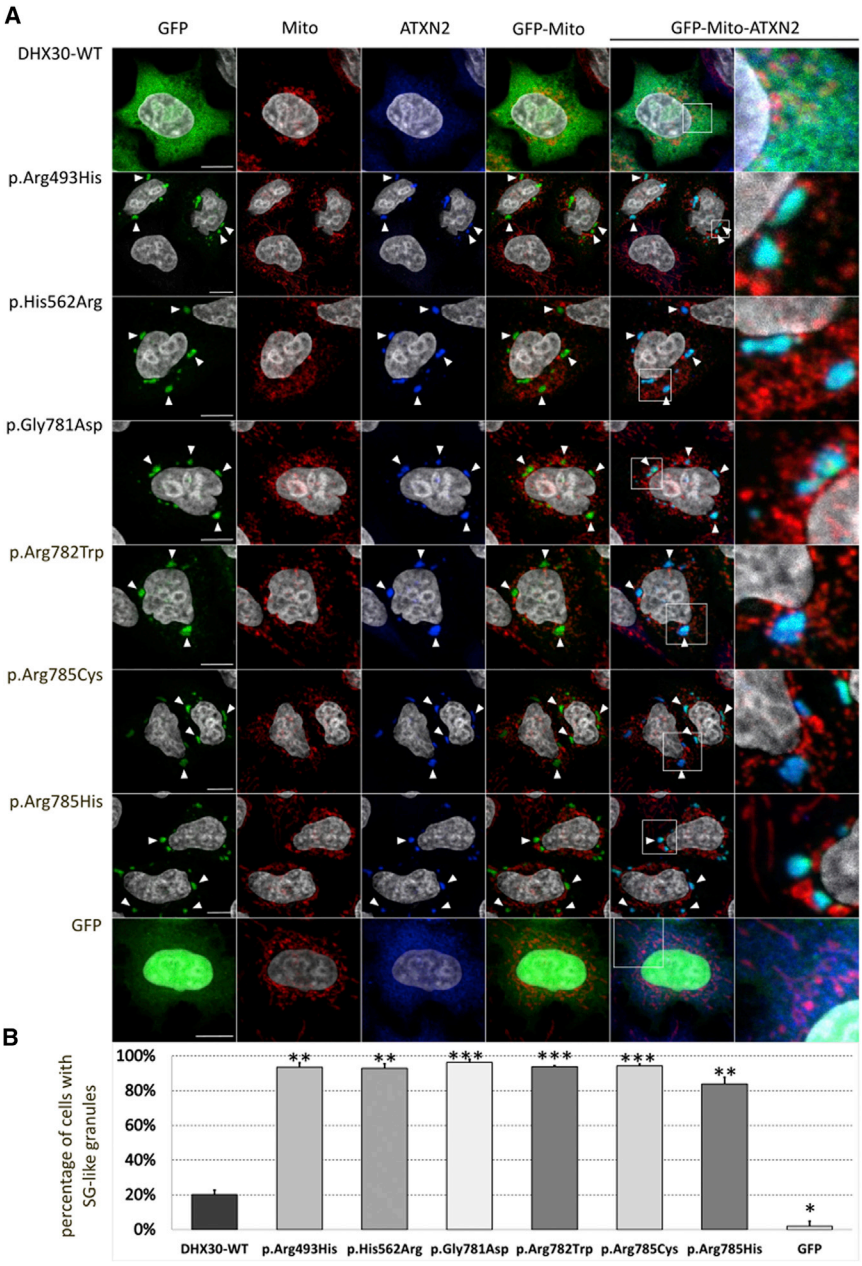

Figure 3. Recombinant Protein Variants of DHX30 Initiate the Formation of SG-like Cytoplasmic Aggregates

(A) Immunocytochemical detection of DHX30-GFP fusion proteins (GFP, green), mitochondria (Mito, red), and endogenous ATXN2 (blue) in transfected U2OS cells. Regions shown at high magnification in the rightmost panels are indicated by boxes. Whereas wild-type DHX30-GFP preferentially resides throughout the cytoplasm and GFP accumulates in nuclei, recombinant protein variants of DHX30 induce the genesis of cytoplasmic foci containing endogenous SG-marker ATXN2 (arrowheads). Nuclei are identified via DAPI staining (gray).

(B) Bar graph indicating the percentage of transfected cells, in which recombinant GFP proteins induce the emergence of SG-like structures. Vertical bars indicate SD. Statistical analysis was performed using unpaired Student's t test to individually compare each protein variant to wild-type DHX30-GFP (*$p < 0.05$; **$p < 0.01$; ***$p < 0.001$; $n > 300$ from two independent transfections).

affecting the putative RNA-binding motif Ia did not alter RNA-dependent ATPase activity of DHX30.

To analyze the impact of p.Arg493His on RNA binding, we performed an RNA immunoprecipitation analysis with transfected HEK293T cells.[18] For this, RNP complexes containing recombinant DHX30-WT or p.Arg493His, respectively, were affinity purified and subjected to quantitative real-time RT-PCR to examine the presence of three distinct putative target mRNAs. Targets were randomly selected from a publicly available eCLIP (enhanced version of the crosslinking and immunoprecipitation) dataset obtained in HepG2 cells (accession ENCSR565DGW), generated by the ENCODE project.[27–29] A detailed view of the respective DHX30 eCLIP hits is shown in Figure S3. We determined that the p.Arg493His amino acid substitution leads to a 9- to 11-fold decrease in the amount of *AES* (MIM: 600188), *B4GAT1* (MIM: 605517), and *MRPL11* (MIM: 611826) mRNAs associated with DHX30. Importantly, only negligible amounts of the three investigated transcripts co-purified with the GFP-mCherry control protein (Figure 2C and Figure S4). These data indicate that the p.Arg493His exchange in DHX30 strongly interferes with its *in vivo* binding capacity to certain target RNAs, yet does not completely abolish RNA recognition.

Next, we investigated the subcellular localization of WT and protein variants of DHX30 in U2OS cells. GFP-tagged DHX30-WT was mostly diffusely localized throughout the cytoplasm (Figure 3) with a slight accumulation in mitochondria, consistent with the distribution of endogenous DHX30 (Figure S5A) and previous findings.[30] In contrast, in the majority of transfected cells all protein variants strongly accumulated in discrete cytoplasmic foci (> 80%; Figure 3), which were identified as SGs via co-labeling with Ataxin-2 (*ATXN2*, MIM: 601517), a well-established SG marker.[31] SGs are cytoplasmic RNPs that form in cells during stress responses when translation initiation rates of most mRNAs are decreased.[32] Remarkably, in response to heat stress endogenous DHX30 also alters its diffuse cytoplasmic localization to accumulate in SGs (Figure S5B). These findings show that independent from exogenous stressors, protein variants of DHX30 exhibit a strongly increased propensity to induce SG assembly compared to DHX30-WT. To further determine if SG formation induced by DHX30 protein variants alters protein synthesis, we monitored global translation rates in transfected versus untransfected U2OS cells. In this assay, puromycin incorporation into newly synthesized peptides directly reflects the translation rate and can be visualized via immunocytochemistry.[33] While expression of all tested

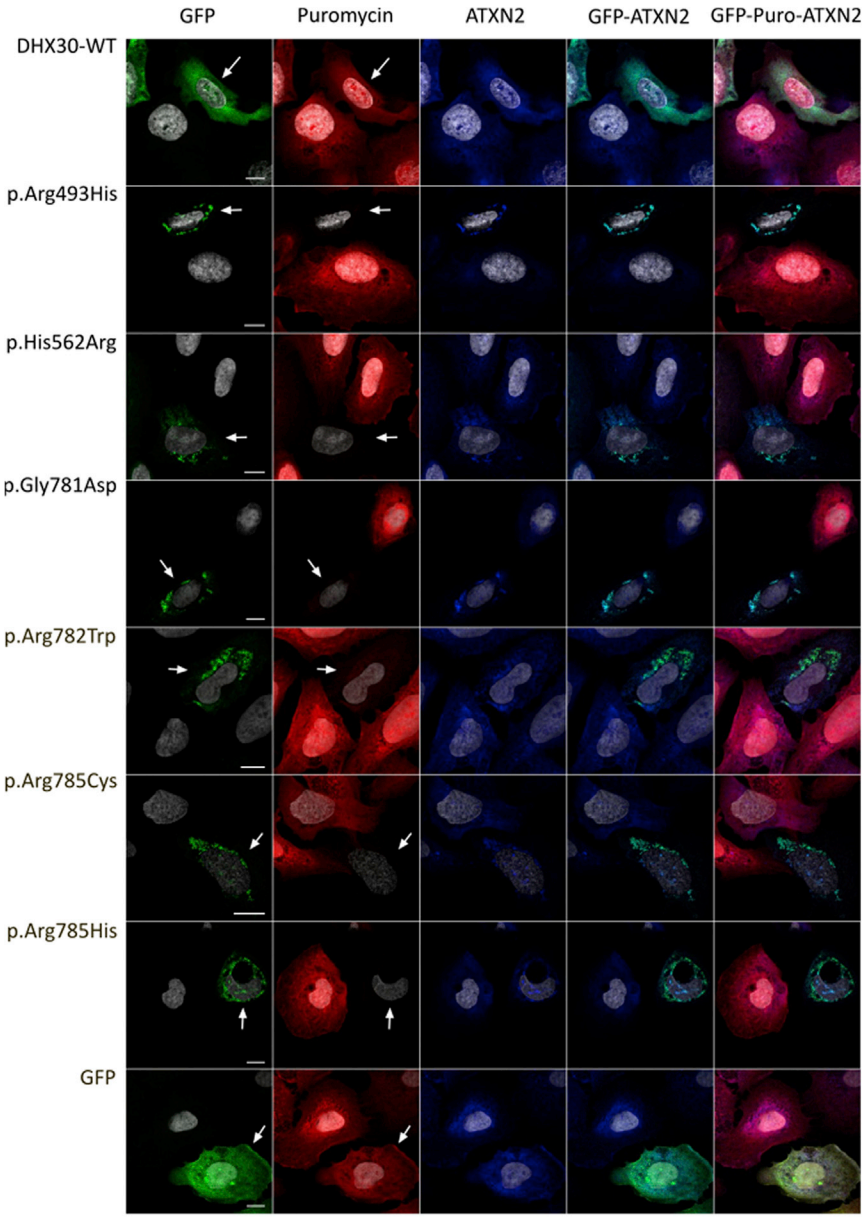

Figure 4. SG Formation Initiated by Protein Variants of DHX30 Selectively Inhibits Global Translation in Transfected U2OS Cells

Puromycin incorporation assay in U2OS cells expressing DHX30-GFP fusion proteins (GFP, green). Translation is monitored by staining against puromycin (Puro, red), SGs are detected by ATXN2 (blue) and nuclei via DAPI staining (gray). While cells expressing wild-type DHX30-GFP or GFP display puromycin labeling comparable to neighboring untransfected cells, puromycin incorporation is strongly diminished in cells expressing recombinant protein variants of DHX30. Arrows indicate transfected cells. Note the correlation between SG assembly and lack of puromycin staining.

recombinant DHX30 protein variants dramatically decreased puromycin incorporation compared to neighboring untransfected cells, puromycin labeling of cells expressing DHX30-WT was similar to that of untransfected cells (Figure 4). Taken together, the above data suggest that protein variants of DHX30 significantly increased the propensity of stress granule formation and thus lead to a global decrease in protein synthesis.

Discussion

Most RHs are involved in several, non-mutually exclusive aspects of RNA metabolism. Similarly, DHX30 was suggested to control different phases of the RNA life cycle as well as ribosome assembly in mitochondria.[30,34,35] However, none of the affected individuals presented here displays clear clinical signs of mitochondriopathies. Thus, it is rather unlikely that the mutations identified here primarily affect mitochondrial function. Actually, our *in vitro* characterization of these mutations has uncovered an additional role for DHX30 related to SG assembly and global translation control. Notably, aberrant SG assembly and clearance with concomitant global translation impairment have been observed in a broad range of neurodegenerative and neurodevelopmental diseases. Examples include amyotrophic lateral sclerosis and frontotemporal dementia (MIM: 612069),[36] spinocerebellar ataxia type 2 (MIM: 183090),[31] Fragile X syndrome (MIM: 300624)[37,38] and Renpenning syndrome (MIM: 309500).[39] Indeed, accurate translation throughout development has recently emerged as a key factor for proper formation and maintenance of complex neural circuits,[40] thereby regulating learning, memory, and behavior. Notably, SGs temporarily arrest mRNA translation upon both exogenous and endogenous stressors.[32] Because the human organism is, even *in utero*, under constant exposure to both endogenous and exogenous stressors, we hypothesize that the mutations identified here generate a chronic condition whereby pervasive and pronounced SG hyper-assembly induces impairments in the local regulation of translation.

Whereas we show a distinct molecular defect for each DHX30 variant with respect to either RNA binding or ATPase activity, one might also speculate that disease-associated sequence alterations in DHX30 could affect protein folding or stability. Indeed, protein levels of GFP-tagged variants are somewhat reduced when compared to WT DHX30, as evident from both fluorescence microscopy (Figures 3 and 4) and western blots of lysates of transfected cells (Figure S6). However, this reduced accumulation level might actually be caused by the induction of SGs which is observed upon expression of *DHX30* variants. As SG formation leads to reduced general translation, DHX30 variants (but not the WT protein) might indeed limit their own production. Given that DHX30-WT is readily incorporated into SGs e.g., upon heat stress, we assume that also the endogenous DHX30 protein is present in SGs upon expression of variant forms of the protein. These

findings might point to a possible dominant negative effect of the mutations identified here.

Interestingly, homozygous deficiency of HelG/DHX30 in mice results in early embryonic lethality, whereas heterozygous mice are apparently normal and fertile.[26] However, no in-depth phenotypic analysis of heterozygous mice, including behavioral tests for learning and memory formation, has been performed up to date. Thus, the so-far published data on DHX30-deficient mice do not allow for a direct comparison of phenotypes with the individuals described here. Nevertheless, they might indicate that the missense mutations described in our study might have a more severe effect than the loss of one copy of the gene.

In conclusion, we report that heterozygous missense mutations in *DHX30* cause a syndrome characterized by GDD, ID, severe speech impairment and gait abnormalities, and highlight the role of proper translation in neurodevelopment.

Supplemental Data

Supplemental Data include five figures and Supplemental Experimental Procedures and can be found with this article online at https://doi.org/10.1016/j.ajhg.2017.09.014.

Data Availability

The identified *DHX30* variants have been deposited to the Leiden Open (source) Variation Database (LOVD) (https://databases.lovd.nl/shared/variants/DHX30/unique) under following accession numbers: 0000195646, 0000195647, 0000195648, 0000195649, 0000195650, 0000195651, 0000195652, and 0000195653. The raw whole-exome sequencing data that support the findings in affected individual cannot be made publicly available for reasons of affected individuals' confidentiality. Qualified researchers may apply for access to these data, pending institutional review board approval. All other data generated or analyzed during this study are included in this published article (and its Supplemental Data files).

Acknowledgments

We thank the family members for their participation and collaboration, Hans-Hinrich Hönck (Institute for Human Genetics, UKE Hamburg) for excellent technical assistance and Tim Kreienkamp (Hamburg) for help with extracting eCLIP data. This work was funded in part by local funding (Forschungsförderungsfonds der Medizinischen Fakultät des Universitätsklinikums Hamburg-Eppendorf [FFM], to D.L.), Deutsche Forschungsgemeinschaft through SPP1935 "Deciphering the RNP Code" (to H.-J.K. and S. Kindler), the US National Human Genome Research Institute (NHGRI)/National Heart Lung and Blood Institute (NHLBI; grant number UM1HG006542 to the Baylor-Hopkins Center for Mendelian Genomics), NHGRI grant to Baylor College of Medicine Human Genome Sequencing Center (U54HG003273) and J.E.P. (K08 HG008986), National Institute of Neurological Disorders and Stroke (NINDS) (R01NS05829 to J.R.L.), the French Ministry of Health and the Health Regional Agency from Poitou-Charentes (HUGODIMS, 2013, RC14_0107). Confocal microscopes were provided by UKE microscopic imaging facility (umif). eCLIP data were produced by the ENCODE consortium (Lab: Gene Yeo at UCSD). Acknowledgments of the DDD Study and a list of C4RCD Research Group members appear in the Supplemental Note. Baylor College of Medicine (BCM) and Miraca Holdings Inc. have formed a joint venture with shared ownership and governance of the Baylor Genetics (BG), which performs clinical exome sequencing. J.R.L. has stock ownership in 23andMe and Lasergen, is a paid consultant for Regeneron Pharmaceuticals, and is a co-inventor on multiple United States and European patents related to molecular diagnostics for inherited neuropathies, eye diseases, and bacterial genomic fingerprinting. K.L.H. is a full time employee of Ambry Genetics.

Received: August 17, 2017
Accepted: September 19, 2017
Published: November 2, 2017

Web Resources

1000 Genomes, http://browser.1000genomes.org/index.html
dbSNP, https://www.ncbi.nlm.nih.gov/projects/SNP/
ENCODE, https://www.encodeproject.org/
Ensembl Genome Browser, http://www.ensembl.org/index.html
ExAC Browser, http://exac.broadinstitute.org/
gnomAD Browser, http://gnomad.broadinstitute.org/
OMIM, http://www.omim.org/

References

1. Linder, P., and Jankowsky, E. (2011). From unwinding to clamping - the DEAD box RNA helicase family. Nat. Rev. Mol. Cell Biol. *12*, 505–516.
2. Jankowsky, E. (2011). RNA helicases at work: binding and rearranging. Trends Biochem. Sci. *36*, 19–29.
3. Laggerbauer, B., Achsel, T., and Lührmann, R. (1998). The human U5-200kD DEXH-box protein unwinds U4/U6 RNA duplices in vitro. Proc. Natl. Acad. Sci. USA *95*, 4188–4192.
4. Umate, P., Tuteja, N., and Tuteja, R. (2011). Genome-wide comprehensive analysis of human helicases. Commun. Integr. Biol. *4*, 118–137.
5. Valentin-Vega, Y.A., Wang, Y.D., Parker, M., Patmore, D.M., Kanagaraj, A., Moore, J., Rusch, M., Finkelstein, D., Ellison, D.W., Gilbertson, R.J., et al. (2016). Cancer-associated *DDX3X* mutations drive stress granule assembly and impair global translation. Sci. Rep. *6*, 25996.
6. Snijders Blok, L., Madsen, E., Juusola, J., Gilissen, C., Baralle, D., Reijnders, M.R., Venselaar, H., Helsmoortel, C., Cho, M.T., Hoischen, A., et al.; DDD Study (2015). Mutations in *DDX3X* Are a Common Cause of Unexplained Intellectual Disability with Gender-Specific Effects on Wnt Signaling. Am. J. Hum. Genet. *97*, 343–352.
7. Sobreira, N., Schiettecatte, F., Boehm, C., Valle, D., and Hamosh, A. (2015). New tools for Mendelian disease gene identification: PhenoDB variant analysis module; and GeneMatcher, a web-based tool for linking investigators with an interest in the same gene. Hum. Mutat. *36*, 425–431.
8. Hempel, M., Cremer, K., Ockeloen, C.W., Lichtenbelt, K.D., Herkert, J.C., Denecke, J., Haack, T.B., Zink, A.M., Becker, J., Wohlleber, E., et al. (2015). De Novo Mutations in *CHAMP1* Cause Intellectual Disability with Severe Speech Impairment. Am. J. Hum. Genet. *97*, 493–500.
9. Küry, S., Besnard, T., Ebstein, F., Khan, T.N., Gambin, T., Douglas, J., Bacino, C.A., Craigen, W.J., Sanders, S.J., Lehmann, A., et al. (2017). De Novo Disruption of the Proteasome

Regulatory Subunit *PSMD12* Causes a Syndromic Neurodevelopmental Disorder. Am. J. Hum. Genet. *100*, 352–363.
10. Ta-Shma, A., Zhang, K., Salimova, E., Zernecke, A., Sieiro-Mosti, D., Stegner, D., Furtado, M., Shaag, A., Perles, Z., Nieswandt, B., et al. (2017). Congenital valvular defects associated with deleterious mutations in the *PLD1* gene. J. Med. Genet. *54*, 278–286.
11. Isidor, B., Küry, S., Rosenfeld, J.A., Besnard, T., Schmitt, S., Joss, S., Davies, S.J., Lebel, R.R., Henderson, A., Schaaf, C.P., et al. (2016). De Novo Truncating Mutations in the Kinetochore-Microtubules Attachment Gene *CHAMP1* Cause Syndromic Intellectual Disability. Hum. Mutat. *37*, 354–358.
12. Deciphering Developmental Disorders, S.; and Deciphering Developmental Disorders Study (2015). Large-scale discovery of novel genetic causes of developmental disorders. Nature *519*, 223–228.
13. Banuelos, E., Ramsey, K., Belnap, N., Krishnan, M., Balak, C., Szelinger, S., Siniard, A.L., Russell, M., Richholt, R., De Both, M., et al. (2017). Case Report: Novel mutations in *TBC1D24* are associated with autosomal dominant tonic-clonic and myoclonic epilepsy and recessive Parkinsonism, psychosis, and intellectual disability. F1000Res. *6*, 553.
14. Kleefstra, T., Kramer, J.M., Neveling, K., Willemsen, M.H., Koemans, T.S., Vissers, L.E., Wissink-Lindhout, W., Fenckova, M., van den Akker, W.M., Kasri, N.N., et al. (2012). Disruption of an EHMT1-associated chromatin-modification module causes intellectual disability. Am. J. Hum. Genet. *91*, 73–82.
15. de Ligt, J., Willemsen, M.H., van Bon, B.W., Kleefstra, T., Yntema, H.G., Kroes, T., Vulto-van Silfhout, A.T., Koolen, D.A., de Vries, P., Gilissen, C., et al. (2012). Diagnostic exome sequencing in persons with severe intellectual disability. N. Engl. J. Med. *367*, 1921–1929.
16. Farwell, K.D., Shahmirzadi, L., El-Khechen, D., Powis, Z., Chao, E.C., Tippin Davis, B., Baxter, R.M., Zeng, W., Mroske, C., Parra, M.C., et al. (2015). Enhanced utility of family-centered diagnostic exome sequencing with inheritance model-based analysis: results from 500 unselected families with undiagnosed genetic conditions. Genet. Med. *17*, 578–586.
17. Eldomery, M.K., Coban-Akdemir, Z., Harel, T., Rosenfeld, J.A., Gambin, T., Stray-Pedersen, A., Küry, S., Mercier, S., Lessel, D., Denecke, J., et al. (2017). Lessons learned from additional research analyses of unsolved clinical exome cases. Genome Med. *9*, 26.
18. Miroci, H., Schob, C., Kindler, S., Ölschläger-Schütt, J., Fehr, S., Jungenitz, T., Schwarzacher, S.W., Bagni, C., and Mohr, E. (2012). Makorin ring zinc finger protein 1 (MKRN1), a novel poly(A)-binding protein-interacting protein, stimulates translation in nerve cells. J. Biol. Chem. *287*, 1322–1334.
19. Tanner, N.K., and Linder, P. (2001). DExD/H box RNA helicases: from generic motors to specific dissociation functions. Mol. Cell *8*, 251–262.
20. Tauchert, M.J., Fourmann, J.B., Lührmann, R., and Ficner, R. (2017). Structural insights into the mechanism of the DEAH-box RNA helicase Prp43. eLife *6*, 6.
21. Caruthers, J.M., and McKay, D.B. (2002). Helicase structure and mechanism. Curr. Opin. Struct. Biol. *12*, 123–133.
22. Martin, A., Schneider, S., and Schwer, B. (2002). Prp43 is an essential RNA-dependent ATPase required for release of lariat-intron from the spliceosome. J. Biol. Chem. *277*, 17743–17750.
23. Tanaka, N., and Schwer, B. (2006). Mutations in PRP43 that uncouple RNA-dependent NTPase activity and pre-mRNA splicing function. Biochemistry *45*, 6510–6521.
24. Lek, M., Karczewski, K.J., Minikel, E.V., Samocha, K.E., Banks, E., Fennell, T., O'Donnell-Luria, A.H., Ware, J.S., Hill, A.J., Cummings, B.B., et al.; Exome Aggregation Consortium (2016). Analysis of protein-coding genetic variation in 60,706 humans. Nature *536*, 285–291.
25. Samocha, K.E., Robinson, E.B., Sanders, S.J., Stevens, C., Sabo, A., McGrath, L.M., Kosmicki, J.A., Rehnström, K., Mallick, S., Kirby, A., et al. (2014). A framework for the interpretation of de novo mutation in human disease. Nat. Genet. *46*, 944–950.
26. Zheng, H.J., Tsukahara, M., Liu, E., Ye, L., Xiong, H., Noguchi, S., Suzuki, K., and Ji, Z.S. (2015). The novel helicase helG (DHX30) is expressed during gastrulation in mice and has a structure similar to a human DExH box helicase. Stem Cells Dev. *24*, 372–383.
27. Van Nostrand, E.L., Pratt, G.A., Shishkin, A.A., Gelboin-Burkhart, C., Fang, M.Y., Sundararaman, B., Blue, S.M., Nguyen, T.B., Surka, C., Elkins, K., et al. (2016). Robust transcriptome-wide discovery of RNA-binding protein binding sites with enhanced CLIP (eCLIP). Nat. Methods *13*, 508–514.
28. Consortium, E.P.; and ENCODE Project Consortium (2012). An integrated encyclopedia of DNA elements in the human genome. Nature *489*, 57–74.
29. Sloan, C.A., Chan, E.T., Davidson, J.M., Malladi, V.S., Strattan, J.S., Hitz, B.C., Gabdank, I., Narayanan, A.K., Ho, M., Lee, B.T., et al. (2016). ENCODE data at the ENCODE portal. Nucleic Acids Res. *44* (D1), D726–D732.
30. Wang, Y., and Bogenhagen, D.F. (2006). Human mitochondrial DNA nucleoids are linked to protein folding machinery and metabolic enzymes at the mitochondrial inner membrane. J. Biol. Chem. *281*, 25791–25802.
31. Nonhoff, U., Ralser, M., Welzel, F., Piccini, I., Balzereit, D., Yaspo, M.L., Lehrach, H., and Krobitsch, S. (2007). Ataxin-2 interacts with the DEAD/H-box RNA helicase DDX6 and interferes with P-bodies and stress granules. Mol. Biol. Cell *18*, 1385–1396.
32. Mahboubi, H., and Stochaj, U. (2017). Cytoplasmic stress granules: Dynamic modulators of cell signaling and disease. Biochim. Biophys. Acta *1863*, 884–895.
33. Schmidt, E.K., Clavarino, G., Ceppi, M., and Pierre, P. (2009). SUnSET, a nonradioactive method to monitor protein synthesis. Nat. Methods *6*, 275–277.
34. Minczuk, M., He, J., Duch, A.M., Ettema, T.J., Chlebowski, A., Dzionek, K., Nijtmans, L.G., Huynen, M.A., and Holt, I.J. (2011). TEFM (c17orf42) is necessary for transcription of human mtDNA. Nucleic Acids Res. *39*, 4284–4299.
35. Antonicka, H., and Shoubridge, E.A. (2015). Mitochondrial RNA Granules Are Centers for Posttranscriptional RNA Processing and Ribosome Biogenesis. Cell Rep. February 12, 2015. https://doi.org/10.1016/j.celrep.2015.01.030.
36. Li, Y.R., King, O.D., Shorter, J., and Gitler, A.D. (2013). Stress granules as crucibles of ALS pathogenesis. J. Cell Biol. *201*, 361–372.
37. Vanderklish, P.W., and Edelman, G.M. (2005). Differential translation and fragile X syndrome. Genes Brain Behav. *4*, 360–384.
38. Gareau, C., Houssin, E., Martel, D., Coudert, L., Mellaoui, S., Huot, M.E., Laprise, P., and Mazroui, R. (2013). Characterization of fragile X mental retardation protein recruitment and dynamics in Drosophila stress granules. PLoS ONE *8*, e55342.
39. Kunde, S.A., Musante, L., Grimme, A., Fischer, U., Müller, E., Wanker, E.E., and Kalscheuer, V.M. (2011). The X-chromosome-linked intellectual disability protein PQBP1 is a component of neuronal RNA granules and regulates the appearance of stress granules. Hum. Mol. Genet. *20*, 4916–4931.
40. Darnell, J.C., and Richter, J.D. (2012). Cytoplasmic RNA-binding proteins and the control of complex brain function. Cold Spring Harb. Perspect. Biol. *4*, a012344.

The American Journal of Human Genetics, Volume *101*

Supplemental Data

De Novo Missense Mutations in *DHX30* Impair Global Translation and Cause a Neurodevelopmental Disorder

Davor Lessel, Claudia Schob, Sébastien Küry, Margot R.F. Reinders, Tamar Harel, Mohammad K. Eldomery, Zeynep Coban-Akdemir, Jonas Denecke, Shimon Edvardson, Estelle Colin, Alexander P.A. Stegmann, Erica H. Gerkes, Marine Tessarech, Dominique Bonneau, Magalie Barth, Thomas Besnard, Benjamin Cogné, Anya Revah-Politi, Tim M. Strom, Jill A. Rosenfeld, Yaping Yang, Jennifer E. Posey, LaDonna Immken, Nelly Oundjian, Katherine L. Helbig, Naomi Meeks, Kelsey Zegar, Jenny Morton, the DDD study, Jolanda H. Schieving, Ana Claasen, Matthew Huentelman, Vinodh Narayanan, Keri Ramsey, C4RCD Research Group, Han G. Brunner, Orly Elpeleg, Sandra Mercier, Stéphane Bézieau, Christian Kubisch, Tjitske Kleefstra, Stefan Kindler, James R. Lupski, and Hans-Jürgen Kreienkamp

Supplemental Note: Case Reports

Individual A is a 5-year-old girl, the only child of unaffected, non-consanguineous French parents of Caucasian European descent. Regarding family history, her mother was diagnosed with multiple sclerosis 13 years ago, her father's twin brother had a history of epilepsy and one of her father's sisters had absence seizures, while one of her maternal uncle presents a intellectual deficiency of unknown etiology. The pregnancy was uncomplicated with normal screening ultrasounds. She had normal birth length (51 cm, +0.7 SD), weight (3100 gram, -0.7 SD) and Occipito-Frontal Circumference (OFC; 33.5 cm, -0.9 SD). She had myoclonic seizures since the age of one month, accompanied by repeated absence seizures. Her milestones of motor development were delayed: she was able to sit independently at 12 months and to walk at 32 months of age. At last thorough clinical assessment, at 3 years and 9 months old, her height was 97 cm (-0.5 SD), her weight was 16 kg (-1.4 SD) and her OFC was 47 cm (-2 SD). Her walking was unsteady with frequent slips and falls. She spoke 20 words. She displayed muscular hypotonia and poor fine motor skills. Toilet training was delayed, and she was unable to feed herself. She experienced constipation and sleep disturbance which required melatonin (5 mg/d) with nonetheless persistent night awakening. She showed attention deficit and had auto-aggressive and hetero-aggressive behaviors, low frustration tolerance and showed hand flapping motor stereotypies. Physical examination revealed no obvious dysmorphic features, save convergent strabismus and relatively broad hands and feet, together with a mild distal joint hyperlaxity, a café-au-lait spot in the left basi-thoracic region, two one-centimeter large hypochromic patches respectively next to the left shoulder blade and at the right side. Left cutaneous plantar reflex response was indifferent, whereas the right one was uncertain. Normal control of voluntary purposeful eye movement ruled out a possible oculomotor apraxia. Brain MRI and metabolic investigations, including serum creatine kinase (SCK) were unremarkable. Electroencephalogram (EEG) was normal, as well as neurotransmitter levels in cerebrospinal fluid. *FMR1*, *RAI1*, *CDKL5*, *MECP2* and *FOXG1* genes sequencing and array-CGH gave normal results. Trio whole exome sequencing (trio-WES), with DNA samples of both unaffected parents and the proband, revealed a *de novo* variant c.1478G>A, p.Arg493His, in *DHX30* (NM_138615.2).

Individual B is a 13-year-old boy, the only child of unaffected, non-consanguineous parents of Dutch ancestry. Family history was non-contributory. He was born after 37 weeks of gestation

with a birth weight of 2660 grams (-0.5 SD). As a baby, he had poor feeding due to hypotonia. Unilateral cryptorchidism was present. Psychomotor development was severely delayed. He was able to walk unsupported at the age of 4 years and spoke his first words at the age of 6 years. Automutilation had been reported at younger age. Esophoria of the right eye and mild hypermetropia were observed. A brain MRI at the age of 8.5 years was normal. At the last examination at the age of 13 years, he was able to speak 4 single words and to walk short distances unsupported, however he required a wheelchair for longer distances. His had an ataxic and dystonic gait and severe hypotonia of the trunk. He has a cheerful behavior, but needs structure and has stereotypies. Food has to be minced because of swallowing difficulties. Physical examination at the age of 13 years showed a low-normal OFC of 52.5 cm (-1.5 SD). His height was normal (0 SD) and his weight was at -1 SD He has facial dysmorphisms including mild facial hypoplasia, prominent crus helix, thin eyebrows, full upper eyelids, full and squared nasal tip and eversion of the lower lip. Examination of the extremities showed broad hands and tapering fingers, broad first digits of the feet, pedes planus and decreased reflexes. His skin is remarkably thin. Previous genetic investigations, consisting of standard metabolic screening, screening for Pitt-Hopkins syndrome (*TCF4*), West syndrome (*ARX*), X-linked alpha-thalassemia with mental retardation (*ATRX*), Rett syndrome (*MECP2*) and a 250k SNP array all gave normal results. Trio-WES, with DNA samples of both unaffected parents and the proband, revealed a *de novo* heterozygous variant c.1478G>A, p.Arg493His, in DHX30 (NM_138615.2).

Individual C is a 6-year-old girl, the first child of unaffected, non-consanguineous parents of Turkish origin. She has a 2.5-year-old brother whose development was uneventful. She was born after an uneventful pregnancy at 40 weeks of gestation with a birth weight of 3190g (-0.67 SD) length of 50cm (-0.77 SD), and a borderline OFC of 34 cm (-0.69 SD). She could roll over at four months and mother reports an unremarkable development until the age of six months, when the girl received a vaccination. Developmental delay, muscular hypotonia, and strabismus first became evident at the age of six months. At the age of 6 years and 3 months she had severe developmental delay with a secondary microcephaly, OFC 49 cm (-1.8 SD), truncal and orofacial hypotonia, poor fine motor skills and joint hyperlaxity. Weight is 25.8kg (+0.9 SD) and length 111cm (-1.7 SD). She cannot walk and is wheelchair-bound. Language development is significantly delayed and limited to a single word: no. She showed attention deficit and had auto-aggressive and hetero-aggressive behaviors and low frustration tolerance. She has strabismus of the right eye, hyperopia and bilateral hearing loss (Brainstem Auditory Evoked

Responses-performed). Facial dysmorphisms including synophrys and epicanthus were observed. Further, she has severe sleep disturbances that did not improve with melatonin treatment. Brain MRI, EEG, extensive metabolic investigations, including serum creatine kinase (SCK), blood lactate and pyruvate levels, as well cerebrospinal fluid (CSF) analysis were unremarkable. Conventional chromosome analysis of lymphocytes, array-CGH, direct sequencing of the *MECP2* and *UBE3A* genes including the methylation of the *UBE3A* locus all gave normal results. Trio-WES, with DNA samples of both unaffected parents and the proband, revealed a *de novo* heterozygous variant, c.1685A->G, p.His562Arg, in *DHX30* (NM_138615.2).

Individual D is a 8-year-old girl, the first child of unaffected, non-consanguineous parents of Yemenite/Tripolitan Jewish descent. She has a younger brother whose development is uneventful. She was last examined at 8 years of age. Pregnancy followed *in-vitro* fertilization, and was otherwise uncomplicated. She was born at 40 weeks gestation with birth weight of 3030 grams (-0.75 SD). All milestones of motor development were delayed: she started to roll over at 12 months of age, and could not yet sit independently nor walk at 8 years. In terms of fine motor development, she tried to feed herself with a spoon and could reach for objects. She had difficulties chewing. She did not speak any words at 8 years, but could choose between 'yes' and 'no' on a touch screen computer (iPad). She is described as a pleasant, quiet, smiling child with no behavioral concerns. Sleep difficulties were apparent; she would lie awake quietly for hours at night. Ocular exam including funduscopic examination was normal other than difficulty with accommodation, for which she required eyeglasses. Hearing was reported as normal, but Brainstem Evoked Response Audiometry (BERA) showed slow conduction in the right brainstem. She did not have outright seizures, although episodes of deep inspirium followed by laughter were suspected as epilepsy-equivalent symptoms. EEG showed multifocal abnormalities. Brain MRI obtained at 15 months of age showed delayed myelination, enlarged ventricles, and cerebellar atrophy. Growth parameters at 8 years of age were height 116 cm (-2.1 SD) and weight 17.2 kg (-2.6 SD). Physical examination revealed a high palate, generalized hypotonia, bruxism, choreiform movements, bilateral single palmar crease, and head lag. Prior work-up included abdominal US, echocardiography, thyroid function tests, lactate, ammonia, plasma amino acids, homocysteine, transferrin isoforms analysis, very long chain fatty acids, urine organic acids, and urine for creatinine and guanidinoacetate were unremarkable. Chromosome analysis, array-CGH, *MECP2* sequencing, and methylation of the *UBE3A* locus all gave normal results. Trio-WES, with DNA samples of both unaffected parents and the

proband, revealed a *de novo* heterozygous variant, c.2342G>A, p.Gly781Asp, in *DHX30* (NM_138615.2).

Individual E is a 17-year-old boy, third child of unaffected, non-consanguineous parents of Caucasian European ancestry. He has two unaffected older sisters. The pregnancy was uncomplicated with normal screening ultrasounds. He was born after 40 weeks of gestation with normal birth length (51 cm, 0 SD), weight (3830 g, +1 SD) and OFC (34.5 cm, 0 SD). He had neonatal hypotonia with poor feeding. Unilateral cryptorchidism and left post-axial hexadactyly of the foot were present. All milestones of motor development were severely delayed: he was able to sit independently at 3 years and to walk at 6 years of age. A brain MRI at the age of 4 years showed cortical atrophy and enlarged ventricles. At the age of 17 years, his height was 165 cm (-1,5 SD), his weight was 55 kg (- 0,75 SD) and her OFC was 54 cm (-1,5 SD). He is still unable to speak and he can walk only short distances. His has an ataxic gait. He has facial dysmorphisms including broad and large eyebrows, eversion of lower eyelids, and orofacial hypotonia. Examination of the extremities showed persistence of fingerpads. He had bruxism. He is described as a pleasant, quiet, smiling boy. However, he displays hetero-aggressive behavior when he is tired or during periods of nervousness. Standard metabolic screening was unremarkable. Previous genetic investigations, including screening for Fragile X Syndrome (*FMR1*), Bardet Biedl syndrome (BBS1-10), intellectual disabilities genes panel (275 genes), analysis of mtDNA common mutations and a 15k SNP array all gave normal results. Trio-WES, with DNA samples of both unaffected parents and the proband, revealed a *de novo* heterozygous variant, c.2342G>A, p.Gly781Asp, in *DHX30* (NM_138615.2).

Individual F is a 14-year-old girl, of unaffected, non-consanguineous parents of Hispanic ancestry. She has one full sibling and three maternal half siblings, all of whom have demonstrated normal development. She was born after 40 weeks of gestation with birth length of 51 cm (-0.65 SD), and weight of 2892 g, (-1.7 SD), further birth history was unremarkable. Developmental delays were noted in the first year of life and no period of normal development occurred. She has had no period of regression. Last physical exam, at the age of 14 years, revealed a small for age young lady who is below the 3rd percentile for all growth parameters. She is still unable to speak. She is non-dysmorphic, hypotonic and hyper-extensible. She requires assistance to walk and her gait is significant for ataxia and dystonia. She also has chorea at rest, and demonstrates persistent hand-wringing. She requires gastrostomy feeding to get adequate calories. Biochemical studies have included the following:

creatine/guanidinoacetate (plasma), urine creatine/guanidinoacetate, alpha aminoadipic semialdehyde (plasma), creatine kinase, serum homocysteine, uric acid, CSF glycine, serum glycine, CSF 5-methyltetrahydrofolate, CSF BH4/neopterin, CSF 5-hydroxyindoleaceticacid/homovanillic acid/3-O-methyldopa, copper (serum), ceruloplasmin, carbohydrate deficient transferrin (mono/di and asialo/di ratio), urine amino screen, serum amino acids , urine organic acids, urine mucopolysaccharides, urine oligosaccharides, very long chain fatty acids, phytanic acid, urine purines/pyrimidines, CSF lactate, serum lactate, all of which were unremarkable. Brain MRI revealed a diffuse volume loss, worsening over time. Her last EEG was moderately abnormal due to the presence of vertex spikes, left posterior temporal spikes and generalized spike and wave bursts. Extended genetic investigations, including *COG8* del/dup analysis, PWS/AS méthylation analysis, *UBE3A* sequencing, *SURF1* sequencing, *CDKL5*, *SLC9A6* sequencing and del/dup analysis, *FOXG1* sequencing, oligoarray testing, *TCF4* sequencing, *BOLA3* sequencing, *FMR1* CGG repeat analysis, analysis of mtDNA common mutations all gave normal results. Trio-WES, with DNA samples of both unaffected parents and the proband, revealed a *de novo* heterozygous variant, c.2344C>T, p.(Arg782Trp), in *DHX30* (NM_138615.2).

Individual G is a 14-year-old girl, the second twin of the second pregnancy of unaffected, non-consanguineous parents. During the pregnancy decreased fetal movement was noted. She has a twin brother and an older brother, both of whom have had normal development. She was born after 35+5 weeks of gestation with a normal birth weight, length and OFC. Directly after birth, she had breathing problems that required resuscitation, and spent the first 10 days of life in a neonatal intensive care unit for feeding difficulties. She received surgery for pressure equalizer (PE) tubes at 8 months. Developmental delays were noted in the first year of life. She learned to walk with 3 years, and is still non-verbal at the age of 14 years. A brain MRI at the age of 5 years revealed delayed myelination. Attention deficit hyperactivity disorder (ADHD) was documented. At the examination at 14 years of age she had an ataxic gait, chronic constipation, moderate anxiety, non-purposeful use of hands, tantrums, screams and vocalizations but no sentences. Facial dysmorphisms included long facies, mandibular prognathism, low set ears, open mouth appearance, and large and wide-spaced teeth. Further, long tapering fingers, flat feet with ankle pronation, and mild scoliosis were noted. Cardiac evaluation was unremarkable. Multifocal epileptiform activity was observed on EEG, however she had no history of seizures. Singleton-WES revealed a heterozygous variant, c.2344C>T, p.Arg782Trp, in *DHX30* (NM_138615.2), shown to be *de novo* through Sanger sequencing in both parents.

Individual H is a 8-year-old girl, the second of two children of unaffected, non-consanguineous parents of Dutch ancestry. Family history was non-contributory. She was born after 41+6 weeks of gestation with a birth weight of 3880 gram (+0.5 SD). As a baby, she had a mild esophageal reflux and was hypotonic. Psychomotor development was severely delayed. A brain MRI at the age of 6 months revealed wide ventricles, frontotemporal cerebral atrophy and delayed myelination. One year later, at the age of 1.5 years, a second brain MRI showed no progression of cerebral atrophy. Myelination had slightly progressed, but was still delayed. Physical examination at the age of 5 years showed a secondary microcephaly, with an OFC of 46 cm (-3 SD). Her height was 104 cm (-1.5 SD) and her weight was 14.5 kg (-2 SD). She has facial dysmorphisms including mild facial hypoplasia, mild synophrys, protrusion of the tongue and eversion of her lower lip. At the last examination at the age of 8 years, she was still not able to speak or to walk. Her development was severely delayed. Her hearing and vision were normal. There was no constipation. She was known to have a high pain threshold. No automutilation had been reported. No epileptic episodes have been noticed. Previous genetic investigations, consisting of standard metabolic screening, screening for Prader-Willi syndrome (methylation 15q11-q13), Rett syndrome (*MECP2*, *CDKL5*, *FOXG1*), Kleefstra syndrome (*EHMT1*), Pitt-Hopkins syndrome (*TCF4*), mitochondrial DNA depletion syndrome (*SUCLA2*, *TK2*, *POLG*), optic atrophy (*OPA1*) and a 250k SNP array all gave normal results. Trio-WES, with DNA samples of both unaffected parents and the proband, revealed a *de novo* heterozygous variant, c.2344C>T, p.Arg782Trp, in *DHX30* (NM_138615.2).

Individual I is 6-year-old girl, the second of two children of unaffected, non-consanguineous parents of Northern/Western European/Honduran descent. Family history was non-contributory. She was born at 37 weeks of gestation with a birth weight of 3175 gram (-0.7 SD). She was noted to have muscular hypotonia and developmental delay since 3 months of age. She had frequent upper respiratory infections. Her eyes used to move to the left or to the right aimlessly. At 2-3 years of age, she developed episodes of rapid breathing, loss of consciousness and jerking movements of the eyes and upper extremities. EEG showed posterior sharp waves bilaterally (probably epileptiform) and generalized slowing. She was started on antiepileptic medicine at 3 years of age. Currently, at the age of 6 years, she has severe hypotonia, severe global developmental delay and generalized joint laxity. She does not walk. She cannot sit without support. She is nonverbal. She does not understand any commands. She smiles all the time and has unprovoked prolonged laughing episodes. She has no purposeful movements of

her hands. She has midline play and hand-wringing stereotypy. She has uneven gaze and strabismus. Her left pupil is more dilated than the right. She has poor eye contact and cannot focus on objects. She has high tolerance to pain and she rarely cries. She eats only pureed food from a bottle. She tolerates only thick-consistency liquids, requiring milk to be with pureed vegetables and food. She choeks on her saliva. A brain MRI at the age of 10 months revealed benign communicating hydrocephalus. Another brain MRI at 3 years of age revealed generalized prominence of the CSF spaces and cerebral atrophy. Physical examination at 6 years of age showed relative macrocephaly, with an OFC of 52.25 cm (+1.3 SD). Her height was 100 cm (-3 SD) and her weight was 15 kg (-2 SD). She has facial dysmorphic features that include a high forehead, thin eyebrows, flat nasal bridge, posteriorly rotated ears, smooth philtrum and thin bow shaped upper lip. She has generalized joint laxity and persistent fetal fingertip pads. Standard metabolic screening including urine organic acids, and transferrin isoform analysis for congenital glycosylation disorder were unremarkable. Previous genetic investigations, including blood chromosomal analysis, SNP whole genome microarray, screening for Prader-Willi syndrome/Angelman syndrome (methylation 15q11-q13), *UBE3A* sequence analysis and deletion duplication study, Rett syndrome (*MECP2*, *CDKL5*, *FOXG1*) including sequencing and deletion duplication studies, Pitt-Hopkins syndrome (*TCF4*), Courtagen's epiSEEK® panel that includes sequencing of 327 genes implicated in seizure disorder, and sequence analysis and deletion testing of the mitochondrial genome all gave normal results. Trio-WES, with DNA samples of both unaffected parents and the proband, revealed a *de novo* heterozygous variant, c.2353C>T, p.Arg785Cys, in *DHX30* (NM_138615.2), and a *de novo* heterozygous alteration c.2969A>C, p.D990A in *SPEN*.

Individual J is a 4 8/12-year-old boy, the fourth of four children of unaffected, non-consanguineous parents of Mexican ancestry. There is no noted family history of neurodevelopmental disorders, and no other siblings in the family are symptomatic. Pregnancy was uncomplicated, however mother noted diminished fetal movement. He was born at 37 weeks of gestation via repeat caesarian section with a birth weight of 3150 grams. He had early feeding difficulties, which were ascribed to a cleft palate, for which he underwent surgery at 9 months of age. He developed a social smile at 2 months and rolled over at 6 months. At 6 months of age, he was referred to a neurologist because of hypotonia. He was found to have strabismus and partial syndactyly of the right toes. Brain MRI at 8 months showed cavum of the septum pellucidum, prominent ventricles and extra-axial spaces, thin corpus callosum, and delayed myelination. A subsequent MRI at 4 years revealed shortened corpus callosum with a

thin body and absent splenium; cavum septum pellucidum et vergae; decreased white matter volume, prominent extra-axial spaces and enlarged third ventricle. On examination, at the age of 4 8/12 years, he was a small, thin, well-appearing boy; his weight was 11.3 kg (-3.5 SD) and head circumference was 47.25 cm (-2.5 SD). He was slightly hirsute, with bushy eyebrows, and had less prominent palmar creases than expected. There was partial cutaneous syndactyly of the 2nd and 3rd toes on the right foot. Heart and lung sounds were normal, and there was no organomegaly. He made eye contact, smiled, was alert and attentive, and followed objects. There was a decrease in facial expression, but he did not have myopathic facies. He was vocal, but did not say any words. His muscle tone was diminished throughout (trunk and limbs) and he slipped through on vertical suspension. He was able to pull to stand, and could reach up with his arms. He was able to crawl; he walked with assistance, but did so on a wide base and was unsteady. He did not have a tremor on reaching for objects. Tendon reflexes were normal at the biceps, triceps, knees and ankles. EEG at 4 years was normal, as was renal ultrasound and echo cardiogram. Expanded newborn screen, karyotype (46XY), chromosomal microarray, test for Smith-Lemli-Opitz syndrome (7-dehydrocholesterol), methylation PCR for Prader-Willi syndrome, plasma amino acids, ammonia, acylcarnitine profile thyroid screen, were all unremarkable. Trio-WES, with DNA samples of both unaffected parents and the proband, revealed a *de novo* heterozygous variant, c.2353C>T, p.Arg785Cys, in *DHX30* (NM_138615.2).

Individual K is a 6-year-old girl, the second child of unaffected, non-consanguineous parents of Dutch ancestry. Family history was non-contributory. She was born at home after 40 weeks of gestation with a birth weight of 2970 grams (-1 SD). She fed slowly but gained enough weight. She was a quiet baby. She roll over at a normal age. At twelve month of age she could not sit independently and a delay in motor development and hypotonia were noted. She was able to walk independently at 5 years of age. By six years of age her walk was wide based and unsteady with her arms flexed and raised. She has no verbal words except for some intonated sounds, but and uses some gestures and sounds to communicate. She can have temper tantrums and frustration intolerance. She has stereotypic movements of her head and hands. She is usually in a good mood and likes to hug. There is no auto mutilation. Eye contact is short. She has hypermobile joints and flat feet. An intermittent esotropia of the left eye was detected. Physical examination at the age of 6 years showed normal biometry. She has mild facial dysmorphisms including mild facial hypoplasia, full upper eyelids, and mild epicanthus. Examination of the extremities showed hypermobile joints and pedes planus. A brain MRI at

the age of 1.5 years showed delayed myelinisation and wide ventricles, probably due to cerebral atrophy. Routine biochemical and metabolic screening were unremarkable. Previous genetic investigations, including screening for SMA (*SMN1*), Fragile X syndrome (*FMR1*), (atypical) Rett syndrome (*MECP2*), Angelman syndrome and a 250k SNP array all gave normal results. The SNP array did show a large copy neutral homozygous region (arr[hg19] 5q31.2q32(137,946,508-149,314,425)x2 hmz (2837 SNPs; 11,4 Mb) possibly caused by a UPD or distant consanguinity. Trio-WES, with DNA samples of both unaffected parents and the proband, revealed a *de novo* heterozygous variant, c.2353C>T, p.Arg785Cys, in *DHX30* (NM_138615.2).

Individual L is a 8-year-old boy, the second child of unaffected, non-consanguineous Caucasian parents. There is no family history of relevance, and there are no concerns about his elder sister. The pregnancy was uncomplicated and he was born at home by normal vaginal delivery at 40 weeks gestation. He was noted to be a floppy, sleepy baby. All milestones of motor development were delayed: sitting at 18 months of age and crawling at the age of 3 years. He could pull to stand and walk with hands held at the age of 6 years. At 8 years of age he was able to take 10 to 15 independent unsteady steps. He remained non-verbal and doubly incontinent at the age of 13 years. He still requires help with feeding. He has always made gradual progress and has never regressed. He is a generally happy child and hand flaps when excited. He has delayed visual maturation, has had surgery for a squint and has been registered as partially sighted. On examination, at the age of 6 years, he is hypotonic with no focal neurological signs. He was microcephalic with a head circumference of 48cm (-3.2 SD). He has some subtle dysmorphic features: short, broad thumbs, relatively large ears, pencilled eyebrows, downslanting palpebral fissures and widow's peak anterior hairline. His facial appearance is hypotonic. Two EEG's have been normal. MRI scan of the brain at the age of 12 months showed prominent ventricles and reduction in the volume of the white matter posteriorly. There was diffuse delay in myelination with particular involvement of the temporal lobes and optic radiation. The optic nerves, chiasm and tracts were extremely thin. The posterior fossa appeared normal. Routine baseline biochemical and metabolic investigations, thyroid function tests, purines and pyrimidines were all unremarkable. Previous genetic investigations, including array-CGH, and direct sequencing of *MEF2C* and *FOXG1* all gave normal results. Trio-WES, with DNA samples of both unaffected parents and the proband, revealed a *de novo* heterozygous variant, c.2354G>A, p.Arg785His, in *DHX30* (NM_138615.2).

Supplemental Figures

Figure S1. Facial phenotype of individuals with *DHX30* associated disorder. Facial images of individual B at the ages of 8.5 and 13 years, individual C at the age of 6 years, individual E from the age of 8 till 16 years, individual F at age of 14 years, individual H at the ages 4 and 8 years, individual I at age 6 years, individual J at the age of 4 years, individual K at age of 4.5 years, and individual L at the age of 6 years.

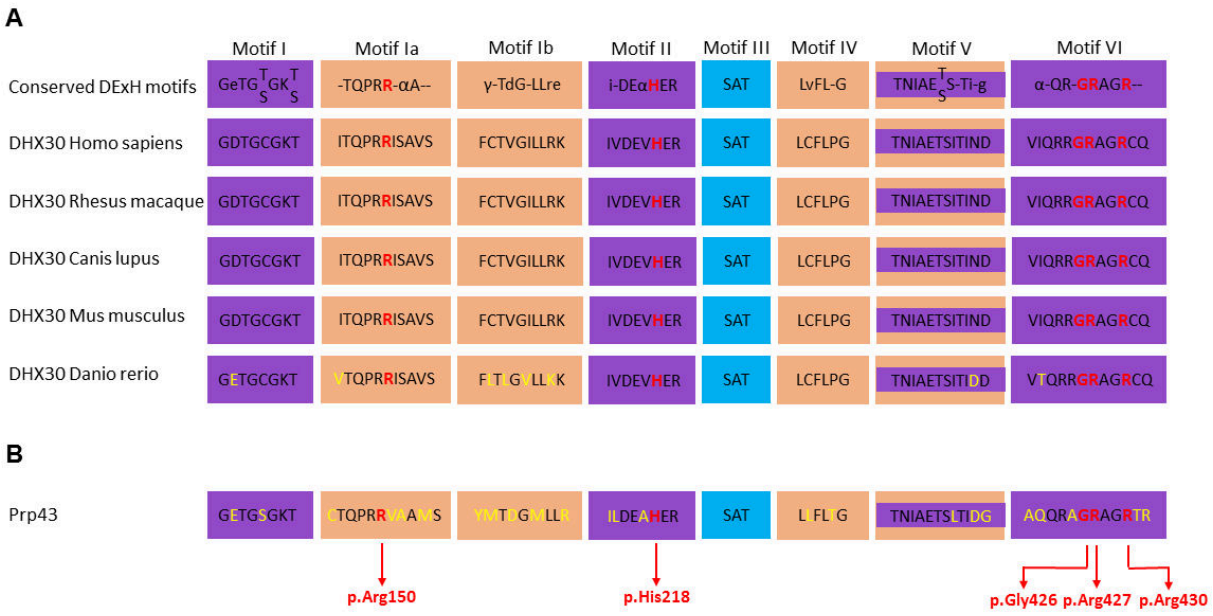

Figure S2. Identified *de novo* missense mutations affect highly conserved residues within helicase sequence motifs. (a) Evolutionary conservation of the motifs within helicase core region. Comparison to other superfamily2 helicases (based on ref.[1]) and DHX30 homologs. The position of the *de novo* mutations identified in this study are shown in red. Non conserved amino acid are shown in yellow. Nucleotide-interacting motifs (I, II and VI) are shown in purple, nucleic acid-binding motifs (Ia, Ib and IV) in orange, motif V, which binds nucleic acid and interacts with nucleotides, in purple and orange, and motif III, which couples ATP hydrolysis to RNA unwinding, in blue. Note that the motifs are evolutionary highly conserved from humans to zebrafish. **(b)** Conserved sequence motifs within helicase core region of the Prp43 in *Saccharomyces cerevisiae*. Note that the residues corresponding to positions of the *de novo* mutations identified in this study, marked with vertical red arrows and shown in red, are highly conserved.

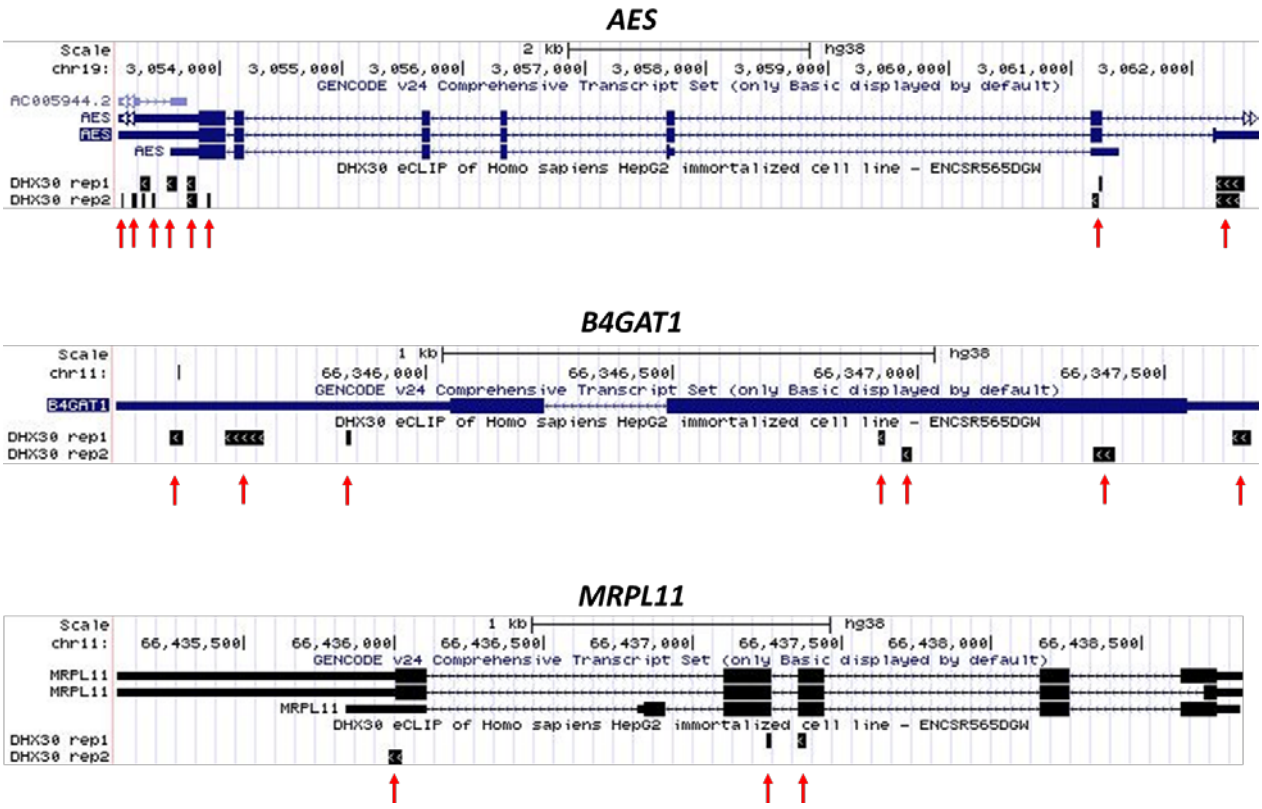

Figure S3. UCSC genome browser view of the DHX30 eCLIP binding sites of *AES*, *B4GAT1* and *MRPL11*. The position of DHX30 binding sites is marked with vertical red arrows (GRCh38/hg38).

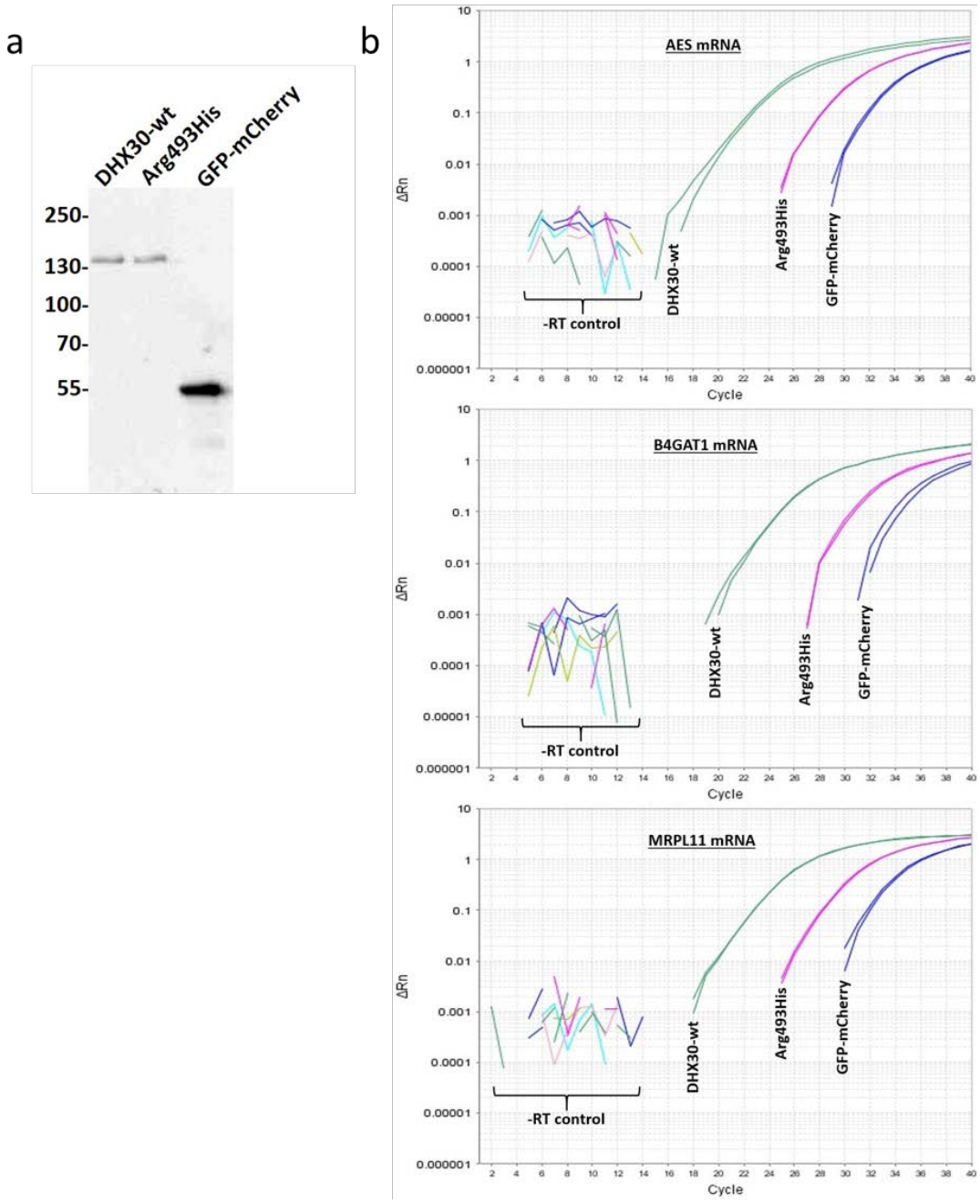

Figure S4. Reduced target mRNA association of p.Arg493His. (a) In a Western blot analysis, anti-GFP antibody detects DHX30-wt, p.Arg493His and GFP-mCherry, respectively, in GFP-Trap_A precipitates obtained from transfected HEK293T cells. Positions of molecular size markers are indicated on the left (in kDa). **(b)** RNAs extracted from GFP-Trap_A precipitates were subjected to gene expression analysis utilizing TaqMan probes specific for human mRNAs. The panel shows representative fluorescence curves for *AES*, *B4GAT1* and *MRPL11* transcripts associated with DHX30-wt (green curves), p.Arg493His (pink) and GFP-mCherry (blue), respectively. Same colour curves represent duplicates. Note that no detectable signal is generated when no reverse transcriptase is included during cDNA synthesis (-RT control).

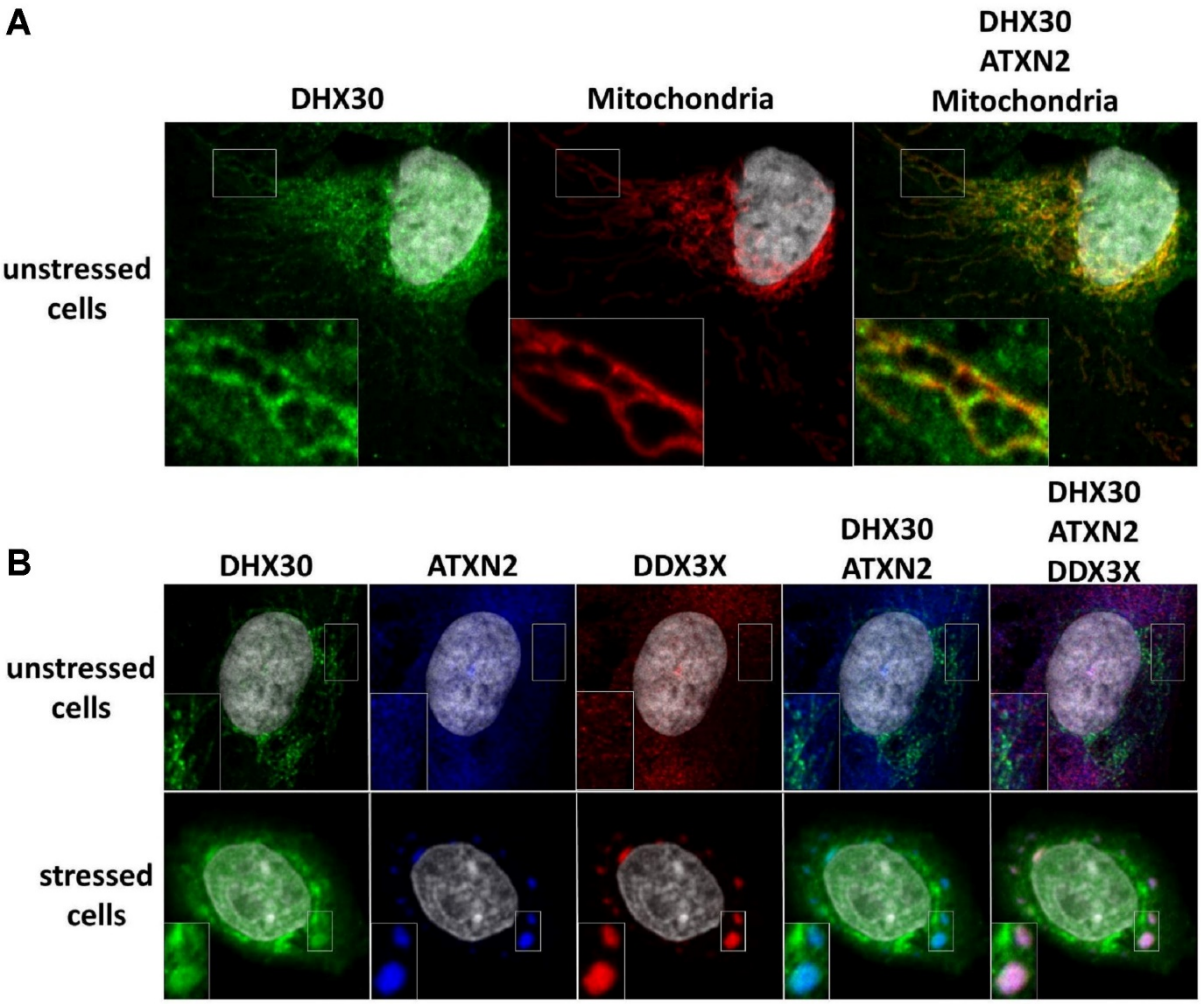

Figure S5. Endogenous DHX30 co-localizes with mitochondria and partially redistributes into SGs in stressed cells. (a) Immunocytochemical detection of endogenous DHX30 (green), mitochondria (red) and ATXN2 (blue). Note that DHX30 strongly co-localizes with mitochondria in unstressed U2OS cells. **(b)** Immunocytochemical detection of endogenous DHX30 (green), DDX3X (red) and ATXN2 (blue). DHX30 partially accumulates in ATXN2- and DDX3X-labelled SGs after stress induction (lower row). Insets inserted in the lower left corner of each panel are magnifications of regions boxed in the same panel. Nuclei are identified via DAPI staining (gray).

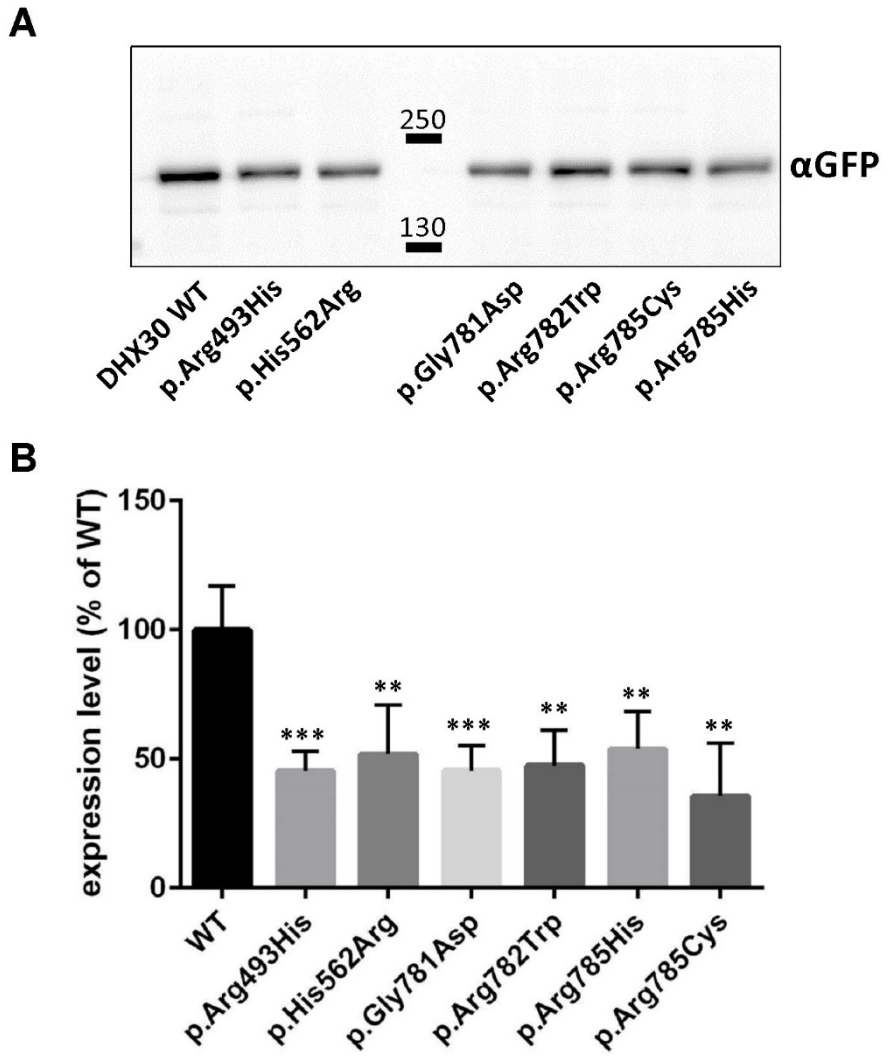

Figure S6. Expression levels of DHX30 variants upon transient transfection in 293 cells. A. Cells expressing WT or variant forms of GFP-tagged DHX30 were lysed and subjected to Western Blot analysis using anti-GFP. B. quantitative analysis, with the expression of DHX30 WT set to 100 %. **, ***, significantly different from WT ($p<0.01$, 0.001, respectively; ANOVA, followed by Dunnett's multiple comparisons test; n=4).

Supplemental Acknowledgments

The DDD study presents independent research commissioned by the Health Innovation Challenge Fund (grant number HICF-1009-003), a parallel funding partnership between the Wellcome Trust and the Department of Health, and the Wellcome Trust Sanger Institute (grant number WT098051). The views expressed in this publication are those of the author(s) and not necessarily those of the Wellcome Trust or the Department of Health. The DDD study has UK Research Ethics Committee approval (10/H0305/83 granted by the Cambridge South REC, and GEN/284/12granted by the Republic of Ireland REC). The research team acknowledges the support of the National Institute for Health Research through the Comprehensive Clinical Research Network.

C4RCD Research Group:

Data analysis and interpretation: Newell Belnap[1], David Craig[1], Matt De Both[1], Matthew Huentelman[1], Madison LaFleur[1], Marcus Naymik[1], Vinodh Narayanan[1], Ryan Richholt[1], Isabelle Schrauwen[1], Ashley Siniard[1], Szabolcs Szelinger[1]

Data analysis and interpretation/wet lab: Chris Balak, Ana Claasen[1], Sampath Rangasamy[1]

Enrollment and Clinical Data: Keri Ramsey[1]

[1]Center for Rare Childhood Disorders, Translational Genomics Research Institute (TGen)

445 N 5th Street, Phoenix, AZ, U.S. 85004

Supplemental references:

1. Tanner, N.K., and Linder, P. (2001). DExD/H box RNA helicases: from generic motors to specific dissociation functions. Mol Cell 8, 251-262.